

Reaction Pathway Discrimination in Alkene Oxidation Reactions by Designed Ti-Siloxy-Polyoxometalates

Teng Zhang,^[a] Albert Solé-Daura,^[b] Hugo Fouilloux,^[a] Josep M. Poblet,^[b] Anna Proust,^[a] Jorge J. Carbó,^{*[b]} and Geoffroy Guillemot^{*[a]}

Titanium complexes of silanol functionalized polyoxometalates (THA)₃[SbW₉O₃₃(RSiO)₃Ti(OⁱPr)] (Ti-SiloxPOMs) catalyze alkene oxidation with *tert*-butyl hydrogen peroxide (TBHP). However catalytic activity and product distribution in the oxidation of allylic alcohols are shown to depend on the steric surrounding generated by the SiloxPOM (*R* = ^tBu, ⁱPr, ⁿPr). Combined experimental and computational studies clarify how steric repulsions between the oxidant (^tBu group) and the surrounding SiloxPOM govern the reaction pathways leading either to oxidation of the alcohol function (*R* = ^tBu) or to alkene

epoxidation (*R* = ⁿPr). Moreover, another consequence of this steric repulsive interactions is that *outer-sphere* mechanisms become competitive with the *inner-sphere* ones (coordination of allylic alcohol), whether for the oxidative dehydrogenation reaction or for the epoxidation reaction. In the case of unfunctionalized olefins (linear and cyclic), we show that reducing the bulkiness surrounding the active site leads to higher conversion to epoxide, emphasizing that these Ti-SiloxPOMs may behave as structural and functional models for metal single-site in Ti-Silicates.

Introduction

Titanium has a long history in oxidation reactions, paved with important dates. In 1980, Sharpless and Katsuki reported the 'first practical method' for enantioselective epoxidation of allylic alcohols by *tert*-butyl hydrogen peroxide.^[1] This achievement was of great synthetic value and led to the following considerations and discoveries: first, the addition of bidentate ligands, such as diols, to titanium alkoxide forms stable chelate complexes that exhibit increased catalytic activity compared to the parent compound (called as "ligand acceleration").^[2] Second, the use of optically active diols, such as dialkyl tartrate, as chiral ligands, induces high enantioselective epoxidation process. Finally, the presence of water is detrimental and epoxidation has to be carried out in the presence of water scavengers, i. e. molecular sieves.

Precisely, substitution of Ti for Si in the framework of hydrophobic zeolites, first reported by Taramasso et al. in 1986,^[3] resulted in the emergence of heterogeneous catalysts of practical use for the liquid-phase oxidation of organic com-

pounds at laboratory and industrial scale, particularly *propene to propene oxide* using H₂O₂ as the terminal oxidant.^[4–7] The catalytic performances of crystalline microporous titanium-silicalites TS-1 are particularly associated to the structural peculiarities of the silica lattice, among which hydrophobicity nature and pore size of the internal channel system are the most relevant,^[8] along with the formation of the reactive hydroperoxo moiety, either on isolated titanium sites^[9,10] or on dinuclear sites.^[11] Indeed, strong physisorption of small apolar substrates is favored whereas water remains outside the pores (in the liquid phase) thus limiting hydrolysis of the isolated active titanium center. Conversely, the hydrophilicity of mesoporous Ti/SiO₂ more often results in leaching process and loss of activity.

We have recently reported that tris-silanol decorated polyoxotungstates (SiloxPOMs) represent interesting ligands to mimic the coordination environment of the tetrahedral defective open-lattice [(≡Si–O)₃Ti(OH)] sites that are expected to prevail in TS-1.^[12,13] They have been built on the polyoxometalate [SbW₉O₃₃]^{9–}, a B-type [Y(W₃O₁₁)₃]^{9–} platform commonly obtained with pyramidal Y heteroatoms (Y = As, Sb, Bi). In reaction with alkyl-trichlorosilanes, the polyoxotungstic framework enables to structure a set of three rigid and preorganized silanol functionalities in a C₃ symmetry that reproduce the chemical and exact geometry environment found in cristobalite (as a model for silica).^[14,15] This significant peculiarity makes these SiloxPOMs realistic models to prepare soluble analogues of titanium(IV)-silicalite oxidation catalysts. An important feature associated to these systems is the possibility to tune the steric hindrance around the metal active site by modifying the size of the alkyl substituents at the silane functionalities. Figure 1 displays the titanium derivatives that we used for these studies: [SbW₉O₃₃(RSiO)₃Ti(OⁱPr)]^{3–} (*R* = ^tBu, ⁱPr, ⁿPr) prepared as tetrahexyl ammonium salts (THA). Decreasing the steric hindrance around the titanium center (from ^tBu to ⁿPr) makes the metal

[a] Dr. T. Zhang, H. Fouilloux, Prof. A. Proust, Dr. G. Guillemot
Institut Parisien de Chimie Moléculaire, IPCM
Sorbonne Université, CNRS
4 place Jussieu
75005 Paris (France)
E-mail: geoffroy.guillemot@sorbonne-universite.fr

[b] Dr. A. Solé-Daura, Prof. J. M. Poblet, Prof. J. J. Carbó
Department de Química Física i Inorgànica
Universitat Rovira i Virgili
Marcel·lí Domingo 1
43007 Tarragona (Spain)
E-mail: j.carbo@urv.cat

Supporting information for this article is available on the WWW under <https://doi.org/10.1002/cctc.202001779>

This publication is part of a Special Collection on "Catalysis in Confined Spaces". Please check the ChemCatChem homepage for more articles in the collection.

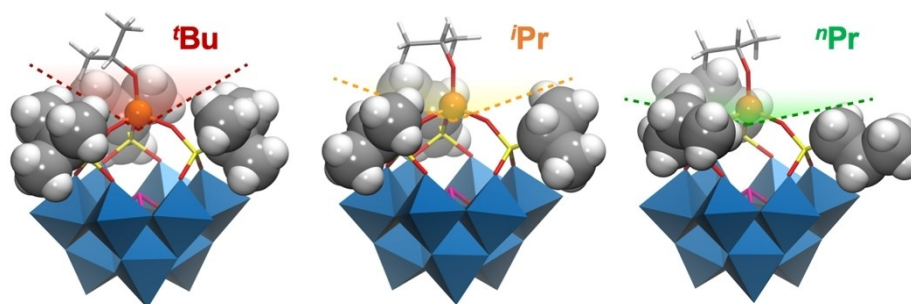


Figure 1. Representation of the structures of $[\text{SbW}_9\text{O}_{33}(\text{RSiO})_3\text{Ti}(\text{O}'\text{R})]^{3-}$ emphasizing the steric crowding generated by the *R* substituents: *R* = *t*Bu (1-*t*Bu); *i*Pr (1-*i*Pr); *n*Pr (1-*n*Pr). The -3 charged compounds are prepared as tetrahexylammonium salts.

center more accessible and therefore allow to modulate its level of confinement in the pseudo-cavity. These systems are therefore well suited to study the impact of the confinement on the activity/selectivity in oxidation reactions.

From our previous studies on the epoxidation of allylic alcohols and unfunctionalized olefins by H_2O_2 , we drew a scheme on the possible mechanisms and set the following conclusions. In the case of allylic alcohol (prenol), the epoxidation proceeds through an *inner-sphere* mechanism, in which the Ti-alcoholate derivative $[\text{Ti}]-\text{OCH}_2\text{CH}=\text{C}(\text{CH}_3)_2$ is the catalytic resting state, whereas in the case of unfunctionalized olefins, an *outer-sphere* mechanism prevails and a Ti-hydroperoxide, $\text{Ti}-(\eta^2\text{-OOH})$, species acts as the resting state and the active species (Scheme 1). Specifically, we observed that in the former case the size of substituents at the Si atom (*t*Bu vs. *i*Pr vs. *n*Pr) has a rather low influence on the conversion/selectivity of allylic alcohols to epoxide whereas it appeared to have a high impact on the accessibility of substrates to the $\text{Ti}-(\eta^2\text{-OOH})$ active species in the case of unfunctionalized olefins. Indeed, decreasing the steric hindrance (from *R* = *t*Bu to *n*Pr) makes energetically accessible an outer-sphere O-transfer to the alkenes but at the same time it also makes favorable the

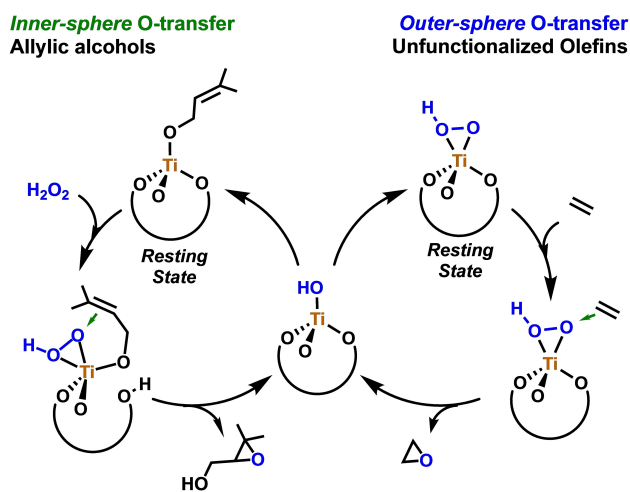
consumption of the H_2O_2 in unproductive ways.^[16] It is worth mentioning here that disproportionation of H_2O_2 (i.e., reaction of two molecules of H_2O_2 at the titanium center) is one major problem that limits efficiency and selectivity of industrial oxidation processes.^[9,10]

In order to avoid the non-productive decomposition of the oxidant, and to draw a complete understanding of the effect of steric hindrance, i.e. the effect of confinement, on the activity and selectivity of oxidation reaction we decided to make use of the more robust *tert*-butyl hydrogen peroxide (TBHP) oxidizing agent. Our results are reported hereafter as a contribution to this *ChemCatChem* special issue 'Catalysis in Confined Spaces'.

Results and Discussion

Titanium complexes

Catalysts preparation. Preparation and characterization of the Ti-SiloxPOM complexes sketched in Figure 1 have already been described in a previous report.^[13] The three complexes $(\text{THA})_3[(\text{SbW}_9\text{O}_{33})(\text{tBuSiO})_3\text{Ti}(\text{O}'\text{Pr})]$, **1-*t*Bu**, $(\text{THA})_3[(\text{SbW}_9\text{O}_{33})(\text{iPrSiO})_3\text{Ti}(\text{O}'\text{Pr})]$, **1-*i*Pr**, and $(\text{THA})_3[(\text{SbW}_9\text{O}_{33})(\text{nPrSiO})_3\text{Ti}(\text{O}'\text{Pr})]$, **1-*n*Pr**, formed as monomers both in solution (NMR and DOSY NMR studies) and in the solid state (X-ray diffraction studies). It is worth mentioning that all our studies (experimental and theoretical)^[12,13] pointed out that the rigid trigonal preorganized set of the silanol functions requires complexing of the metal ion in a constrained pseudo-tetrahedral C_{3v} geometry, and thus makes difficult its coordination sphere expansion. This is in sharp contrast with most commonly reported model systems, and particularly the polyhedral oligomeric silsesquioxanes series, where titanium(IV) can accommodate coordination numbers ranging from 4 to 6.^[17,18] NMR studies in solution also showed that hydrolysis of $[\text{SbW}_9\text{O}_{33}(\text{RSiO})_3\text{Ti}(\text{O}'\text{Pr})]^{3-}$ leads to the formation of a μ -oxo bridged dimer $\{[\text{SbW}_9\text{O}_{33}(\text{RSiO})_3\text{Ti}]_2\text{O}\}^{6-}$ (DOSY NMR and X-ray studies) in which the titanium ion retains its 4 coordination number. When using decane solution of TBHP as oxidizing agent we thus completely avoid the presence of water and hydrolysis process. In that case, complexes **1** very nicely model well-defined monomeric single-sites at a silica surface.^[19]



Scheme 1. Two different pathways for alkene epoxidation with H_2O_2 catalyzed by Ti-SiloxPOM complexes.

Catalytic conditions. In view of our previous studies with aqueous H_2O_2 , we anticipated the formation of a $\text{Ti}(\eta^2\text{-OO}^t\text{Bu})$ moiety during the reaction of **1** with TBHP in acetonitrile. Some of us previously reported that the energy barriers for the O-transfer promoted by $[\text{TM}](\eta^2\text{-OO})$ peroxy species correlate with the energy of the O–O σ antibonding orbital, as a descriptor of the electrophilic character of the peroxy group. On the other hand, in $[\text{TM}](\eta^2\text{-OOH})$ hydroperoxy compounds the energy barriers do not follow a clear trend with the electrophilicity of the oxidant; but instead, they correlate with the strength of the Ti–O $_{\alpha}$ bond.^[20] In this case, although both the Ti–O $_{\alpha}$ and the energy of the $\sigma^*(\text{O–O})$ orbital in the $[\text{Ti}](\eta^2\text{-OO}^t\text{Bu})$ species are rather alike to those of $[\text{Ti}](\eta^2\text{-OOH})$ (see Table S1), higher temperatures were required to achieve the oxidation of alkenes using TBHP as oxidant, suggesting that in this case, steric effects induced by the presence of a ^tBu in the structure of the oxidant may govern the reaction rate while the electronic effects and the strength of the Ti–O bond play a secondary role. Specifically, we proceeded at 65 °C in dry acetonitrile.

(Ep)oxidation of allylic alcohols

Figure 2 (and Table S2) gathers significant results that we obtained in the oxidation of 3-methyl-2-buten-1-ol, an allylic alcohol, with decane solutions of TBHP in acetonitrile at 65 °C catalyzed by complexes $(\text{THA})_3[\text{SbW}_9\text{O}_{33}(\text{RSiO})_3\text{Ti}(\text{O}^i\text{Pr})]$ ($\text{R} = ^t\text{Bu}, ^i\text{Pr}$ or ^nPr).

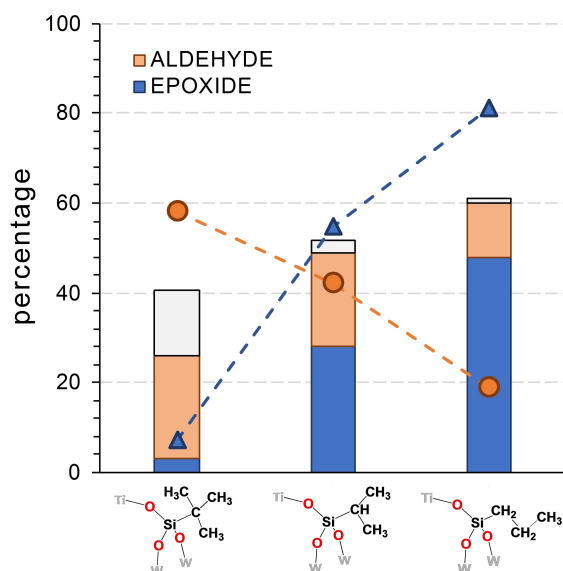


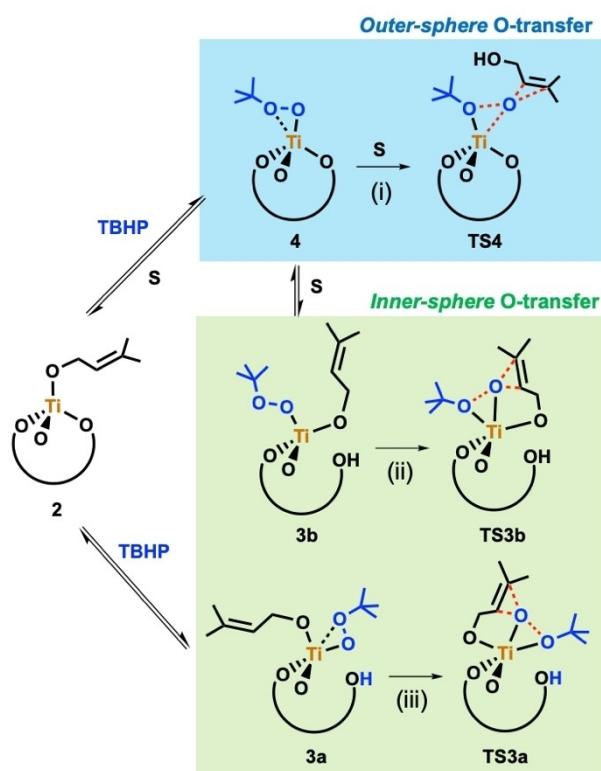
Figure 2. Representation of the formation of oxidized products (*y* axis), i.e., 3-methyl-2-buten-1-ol-oxide (blue), 3-methyl-2-butenal (orange) and undefined products (light gray) after 22 h of reaction at 65 °C in acetonitrile with $[\text{catalyst}] = 2.6 \text{ mM}$, $[\text{3-methyl-2-buten-1-ol}]_0 = [\text{TBHP}]_0 = 0.26 \text{ M}$. From the left to the right, the size of the substituent at the silicon atom decreases: $\text{O}_3\text{Si}^t\text{Bu}$, $\text{O}_3\text{Si}^i\text{Pr}$, $\text{O}_3\text{Si}^n\text{Pr}$. The curves (dashed lines) represent the evolution of selectivity (%) for 3-methyl-2-buten-1-ol-oxide (blue) and 3-methyl-2-butenal (orange).

From these results different trends can be highlighted. First, the less bulky the *R* substituent, the more the conversion. This tends to show that the mechanism *does not* necessarily follow an *inner-sphere* mechanism, but rather an *outer-sphere* mechanism, for which better conversion and selectivity were expected when decreasing the steric hindrance.^[13] This is however not the most striking result. If steric repulsions hamper the formation of epoxide (left column) then oxidation of alcohol mostly takes place and selectivity for the aldehyde 3-methyl-2-butenal increases (Figure 2, orange dashed line). Finally, decreasing the bulkiness at the silicon atom favors epoxidation of olefin versus alcohol oxidation (blue dashed line), the reaction becoming highly selective towards these two products. When using cumyl hydroperoxide (CHP) in place of TBHP as the oxidant, similar trends in selectivity were observed (Table S2).

A first question that arises is whether the formation of the oxidized products is centered on the titanium or not. As we learned from our previous studies in aqueous media, i.e. using aqueous hydrogen peroxide solutions,^[12] increasing the temperature may promote partial decomposition of SiloxPOMs and favor oxidation processes through a well-established metal-peroxide process.^[21–27] Nonetheless, when using TBHP the absence of water prevents any hydrolysis of the POM hybrids. As a controlled experiment we carried out the epoxidation of 3-methyl-2-buten-1-ol by TBHP using the SiloxPOM without titanium center, $(\text{THA})_3[\text{SbW}_9\text{O}_{33}(\text{BuSiOH})_3]$, in the same catalytic conditions than reported in Figure 2. No conversion to epoxide was observed, thus confirming the absence of degradation of the SiloxPOM scaffold. However, significant amount of aldehyde formed, which indicates that the polyoxotungstic framework itself may promote the oxidation of the alcohol function (see Table S1). Thus, whereas epoxidation can be clearly assigned to a titanium centered process, the latter oxidation of the alcohol may proceed either through an heterolytic path oxidation process centered on the titanium (as reported for heterogeneous TS-1) or through an homolytic path made possible by the electron acceptor properties of the POM scaffold. These two different options will be discussed by means of computational studies in the forthcoming part.

Computational characterization of the mechanism for allylic alcohol epoxidation

In order to rationalize the experimental results and to understand how the substituents of Ti-SiloxPOM catalysts affect the oxidation activity and selectivity with TBHP, we next performed computational investigations (see Computational Details). Based on our previous computational studies on the epoxidation with H_2O_2 by Ti-SiloxPOM catalysts,^[13] as well as related studies on other Ti- and transition metal-substituted polyoxometallates,^[20,28–34] we can define 3 possible pathways for the epoxidation of allylic alcohols with TBHP (see Scheme 2). Pathway (i) consists in an outer sphere O-transfer from the $[\text{Ti}](\eta^2\text{-OO}^t\text{Bu})$ species; whereas mechanisms (ii) and (iii) involve inner-sphere transition states in which both the oxidant and the



Scheme 2. Possible mechanisms for the epoxidation of allylic alcohols by Ti-SiloxPOMs. The S label stands for a substrate molecule.

substrate are coordinated to the Ti center after promoting the protolytic cleavage of one of the Ti-OSi bonds.

Figure 3 shows the free-energy profile for the epoxidation of 3-methyl-2-buten-1-ol with TBHP by $1\text{-}^i\text{Bu}$, and compares key values with those of the corresponding H_2O_2 reactant. Figure 4 collects the structures of the transition states for the O-transfer step associated to the three pathways described above. The Ti-isopropoxy precursor $1\text{-}^i\text{Bu}$ was not included in the profile since we have previously shown by means of experimental and computational techniques that its formation during the course of the reaction is unlikely due to the low concentration of both the catalyst and $i\text{PrOH}$ and the higher stability of the Ti-alcoholate species **2**,^[12,13] which represents the resting state of the catalytic cycle. The interaction of **2** with TBHP can lead to two different processes: the insertion of the OH group of the oxidant into a Ti-OSi bond (TS_{2-3a}) causing a partial detachment of the Ti from the structure of the catalyst and yielding species **3a**, in which both the $\eta^2\text{-OO}^i\text{Bu}$ and the substrate remain coordinated to Ti; or a ligand exchange (TS_{2-4}) to generate the $[\text{Ti}](\eta^2\text{-OO}^i\text{Bu})$ species **4** releasing the allylic alcohol to the solvent. Both processes take place through similarly smooth free-energy barriers (14.4 and 15.5 kcal mol⁻¹, respectively) and the formation of both intermediates **3a** and **4** is slightly endergonic (by 3.1 and 3.7 kcal mol⁻¹, respectively). Figures S1 and S2 show the optimized geometries for reaction intermediates and for the transition states that connect them. The back-side approach of the double bond to the $\eta^2\text{-OO}^i\text{Bu}$ moiety in **3a** promotes the inner sphere O-transfer through TS_{3a} , path (iii) in Scheme 2, resulting in a high, overall free-energy barrier of

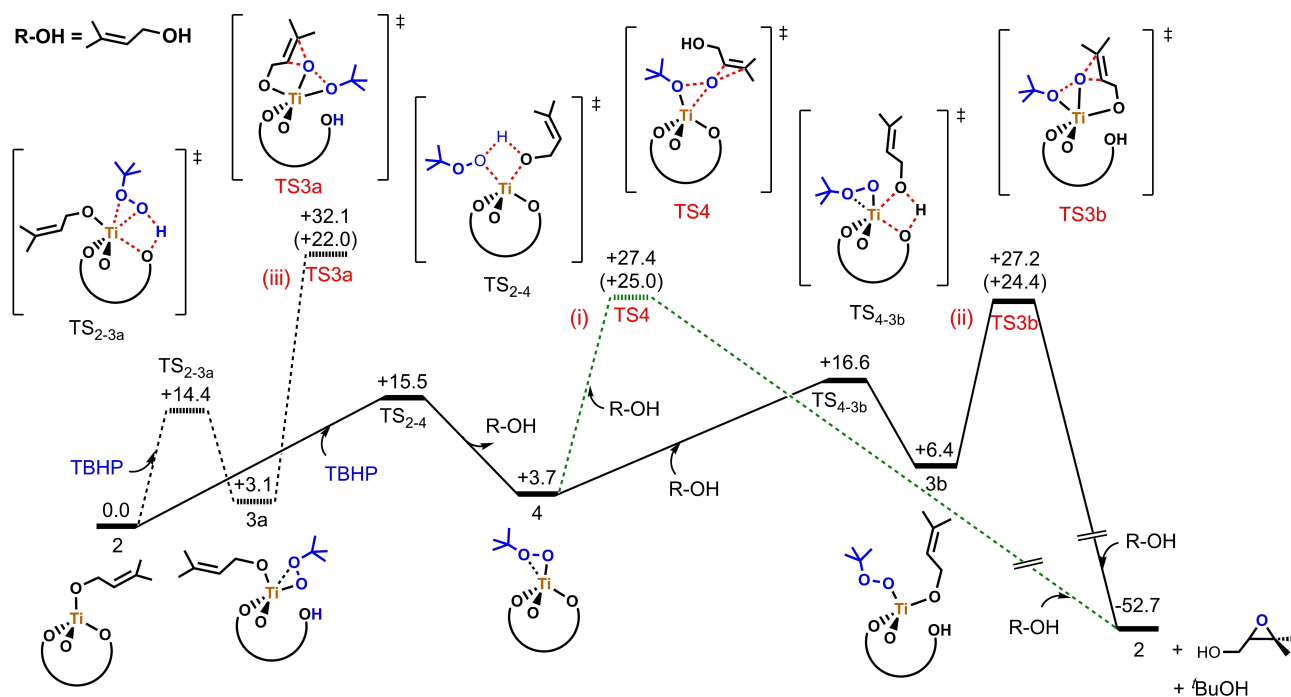


Figure 3. Gibbs free-energy profile (kcal mol⁻¹) for the epoxidation of 3-methyl-2-buten-1-ol catalyzed by $1\text{-}^i\text{Bu}$. Black solid lines represent the inner-sphere mechanism (ii), whereas green and black, dashed lines are associated to the outer-sphere pathway (i) and the inner-sphere pathway (iii), respectively. For comparison, values in parenthesis correspond to the relative free energies associated to analogous transition-state structures using H_2O_2 as oxidant instead of TBHP.

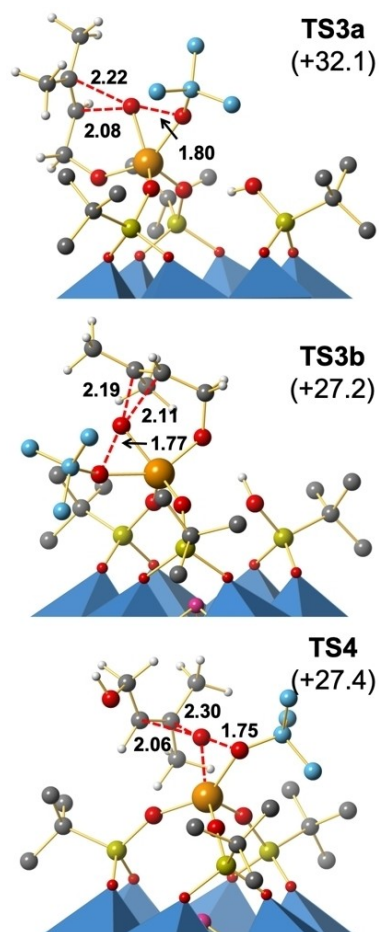


Figure 4. DFT-optimized structures for **TS3a**, **TS3b** and **TS4** included in the reaction profile of Figure 2. Main distances are shown in Å and relative free-energies are given in kcal mol⁻¹. For clarity, hydrogen atoms of ^tBu groups are omitted and carbon atoms of the oxidant are colored in light blue.

32.1 kcal mol⁻¹ from the resting state. Thus, this pathway is prohibitively high in energy for the 1-^tBu catalyst, although as discussed below, it becomes accessible to other catalytic structures bearing smaller groups in the silanol functions. On the other hand, species **4** can directly promote the transfer of the electrophilic alpha oxygen in an outer-sphere fashion, path (i) in Scheme 2, through **TS4** (Figure 4). This process involves a lower overall free-energy energy barrier of 27.4 kcal mol⁻¹ that can be overcome at the experimental temperatures.

Alternatively, intermediate **4** can re-incorporate a molecule of substrate through **TS_{4-3b}** (see Figure 3) overcoming a smooth

barrier of 12.9 kcal mol⁻¹ to give species **3b**, which bearing a η^1 -OO^tBu group, is somewhat less stable than its configurational isomer **3a**. Nonetheless, species **3b** allows the inner-sphere O-transfer through pathway (ii), which involves the formation of the transition state **TS3b** (Figure 4). The overall free-energy barrier associated to pathway (ii) is 27.2 kcal mol⁻¹, being rather similar to that computed for the outer-sphere mechanism (i) (27.4 kcal mol⁻¹). Thus, we concluded that the epoxidation of allylic alcohols catalyzed by 1-^tBu might take place either through outer- or inner-sphere O-transfer mechanisms (paths (i) and (ii), respectively). Also, the height of the overall free-energy barriers is in good agreement with the low experimental conversion towards the epoxide product reported for this catalyst (see Figure 2 and Table S2). Finally, the formation of the epoxide confers to the reaction a strongly exergonic character (by ca. 50 kcal mol⁻¹; see Figure S3) and the regeneration of the resting state to close the catalytic cycle proceeds downhill through several proton transfer and ligand-exchange steps that occur straightforwardly without affecting the overall reaction kinetics as discussed in detail previously.^[13]

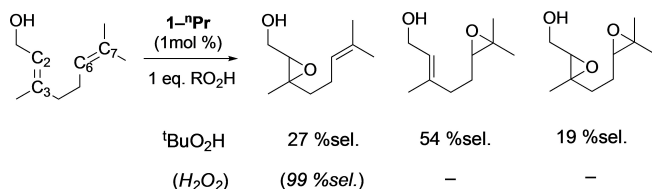
The comparison between the free-energy barriers obtained using TBHP and H₂O₂ (values in parenthesis in Figure 3) as oxidants reveals important features about the reactivity of these compounds. As expected from the higher temperatures that are needed to oxidize alkenes with TBHP, reaching transition state structures for the oxygen transfer to the double bond is more energy-demanding regardless the mechanism. Importantly, whereas the inner-sphere pathway (iii) is clearly favored in the oxidation of allylic alcohols with H₂O₂ due to the release of strain around the Ti center in the TS geometry,^[13] both the inner- and outer-sphere O-transfer mechanisms (paths i) and ii)) become close in energy when using TBHP. This indicates that the steric impact induced by the bulkiness of the ^tBu group of the oxidant is especially important in inner-sphere mechanisms and in turn, can play a crucial role affecting the competition between reaction pathways. In fact, the steric clash between the ^tBu group of the oxidant and other groups of the catalyst and substrate can be appreciated in **TS3a** (see Figure 4; and Figure S4 for more details), which is the most favorable TS in the case of H₂O₂ but is ca. 10 kcal mol⁻¹ higher in energy when using TBHP; in contrast with other paths that are only shifted up by <3 kcal mol⁻¹ (see Figure 3).

Influence of substituents bulkiness in the epoxidation of allylic alcohols

Next, aiming to evaluate how inner- and outer-sphere epoxidation pathways are influenced by steric effects of catalyst substituents, we computed the overall free-energy barriers (from the resting state to **TS3a**, **TS3b** and **TS4**) for the experimentally tested 1-ⁱPr and 1-ⁿPr catalysts, represented in Figure 1. Table 1 compiles the obtained barriers and compares them with those related to 1-^tBu. It has to be pointed out that for R=ⁱPr and ⁿPr the resting state corresponds to a structure analogous to that of **2** but in which a molecule of TBHP is loosely coordinated to Ti through a lone pair of the alpha

Table 1. DFT-derived overall free-energy barriers for the epoxidation of 3-methyl-2-buten-1-ol with TBHP using 1-*R* (*R* = ^tBu, ⁱPr and ⁿPr) catalysts.

Cat. (1- <i>R</i>)	$\Delta G^{\ddagger}_{\text{overall}}$ [kcal mol ⁻¹]		
	Outer-sphere Path (i)	Inner-sphere Path (ii)	Path (iii)
1- ^t Bu	27.4	27.2	32.1
1- ⁱ Pr	25.5	24.3	27.4
1- ⁿ Pr	22.7	23.8	23.1



Scheme 3. Selectivity in the oxidation of geraniol with TBHP catalysed by $(\text{THA})_3[\text{SbW}_9\text{O}_{33}(\text{PrSiO})_3\text{Ti}(\text{O}^n\text{Pr})]$, $1\text{-}^n\text{Pr}$. The carbon atoms of the two double bonds in the starting geraniol are intentionally labelled for clarity.

oxygen (see Figure S5), conferring to the Ti center a distorted trigonal bipyramid geometry. This species lies 4.0 and 2.1 kcal mol⁻¹ below **2** for R = ⁿPr and ⁿPr, respectively and thus, the overall free-energy barriers reported in Table 1 were calculated as the energy difference between this structure and the different transition states. All the attempts of characterizing this species for $1\text{-}^t\text{Bu}$ catalyst failed because the TBHP molecule decoordinates from the Ti during the geometry optimization due to steric repulsions with the ^tBu groups of the catalyst. In agreement with the experimental results, decreasing the bulkiness of the R substituent prevents the steric repulsions in TS structures decreasing the height of the free-energy barriers (going down in Table 1). Particularly interesting, we found a mechanistic shift moving from bulky to small substituents, as for R = ⁿPr the outer-sphere oxidation pathway becomes competitive with inner-sphere ones.

To further support this mechanistic shift towards an outer-sphere we carried out the oxidation of geraniol (trans-3,7-dimethyl-2,6-octadien-1-ol) using $1\text{-}^n\text{Pr}$. In the outer-sphere path a preference for the more nucleophilic 6,7 bond ($E_{\pi_{\text{C}=\text{C}}} = -8.91$ eV) rather than for the 2,3 one ($E_{\pi_{\text{C}=\text{C}}} = -9.04$ eV) is expected, whereas in the inner-sphere path a full selectivity for 2,3-epoxy is expected. As shown in Scheme 3, the oxidation of geraniol with TBHP affords a higher selectivity for the 6,7-epoxy geraniol rather than for the 2,3-epoxy geraniol, indicating that indeed, the outer-sphere path governs the reactivity of $1\text{-}^n\text{Pr}$ with TBHP. This result contrasts with that of the epoxidation of geraniol with H_2O_2 , in which a 99:1 selectivity was observed for the 2,3-epoxy geraniol according to the greater accessibility of inner-sphere mechanisms (see Figure 3); and it is by far representative of the importance of the size of the R group at the peroxide entity (H vs ^tBu). We carried out additional calculations with geraniol to evaluate whether our mechanistic

Table 2. DFT-derived overall free-energy barriers for the epoxidation of the 2,3 and the 6,7 double bonds in geraniol with TBHP catalyzed by $1\text{-}^n\text{Pr}$.

Path	$\Delta G^\ddagger_{\text{overall}}$ [kcal mol ⁻¹]	Probability of reacting through these paths at 65 °C
2,3-inner; path (ii)	26.2	31 %
2,3-inner; path (iii)	24.4	
2,3-outer; path (i)	25.0	
6,7-outer; path (i)	23.6	69 %

scenario is capable of explaining the selectivity observed in this substrate. Table 2 collects the overall free-energy barriers obtained for the epoxidation of geraniol using TBHP and the $1\text{-}^n\text{Pr}$ catalyst. In agreement with experimental selectivity, calculations revealed that the outer-sphere O-transfer to the 6,7 double bond is slightly more favorable than the fastest pathway to oxidize the 2,3-double bond. In fact, the 69:31 ratio derived from DFT barriers is rather consistent with the experimental 2:1 product distribution.

Origin of chemoselectivity: Aldehyde vs. epoxide formation

Figure 2 features a product selectivity discrimination as a function of the bulkiness at the Ti-SiloxPOM. The oxidation of allylic alcohols to unsaturated aldehydes by titanium silicalites – as a specific case of oxidation of alcohol to ketones – is considered to proceed through an oxidative dehydrogenation reaction. Maspero and Romano on the basis of kinetic analysis, have proposed that oxidation of alcohol in heterogeneous TS-1 proceeds following a concerted mechanism in which an irreversible H-transfer from the α -carbon atom of the alcoholate towards the distal oxygen of Ti–OOR occurs in a transition state consisting of a six-membered ring (related to the chair-like conformation in Oppenauer oxidation).^[35] In this context, intermediates **3 a** and **3 b** (Scheme 2) can be considered as ideal candidates to promote this heterolytic dehydrogenation mechanism. However, we were unable to find any inner-sphere pathway that can be energetically competitive to the epoxidation path when using $1\text{-}^t\text{Bu}$ (see Scheme S1). Alternatively, we were able to characterize a lower-energy reaction mechanism consisting in an *outer-sphere*, heterolytic hydrogen abstraction from the allylic carbon of the substrate by the electrophilic α -oxygen of the peroxide group in **4**, provoking the cleavage of the O–O bond and yielding the corresponding cationic allylic alcohol. Figure 5 shows the transition state structure (**TS_{ald}**), and Scheme 4 shows the overall, novel mechanism proposed in this work. Here the nucleophilic character of the allylic C–H attack is manifested through the NPA electron density transfer in the transition state **TS_{ald}**, about 0.4 e, from the allylic alcohol to the peroxide complex. In agreement with the experimental preference for the aldehyde product, the overall free-energy barrier

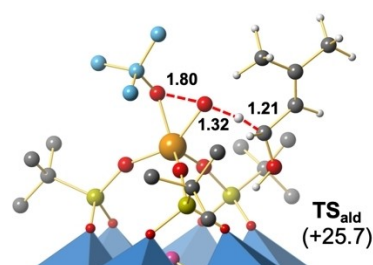
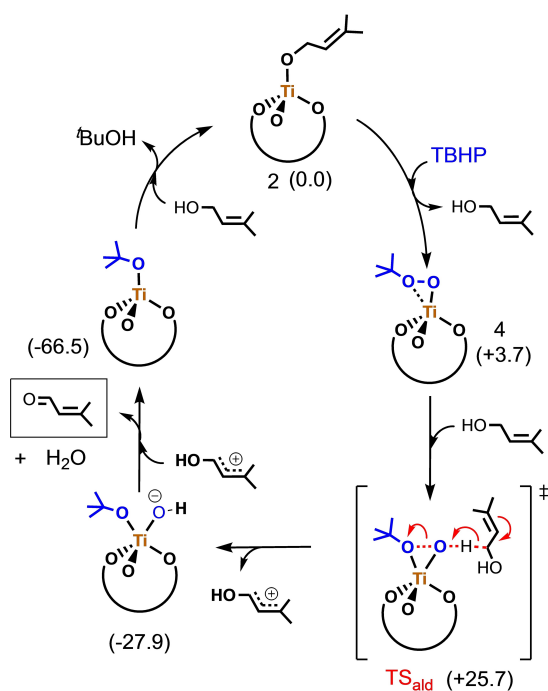


Figure 5. DFT-optimized structure for **TS_{ald}** responsible for the formation of the aldehyde by-product catalyzed by $1\text{-}^t\text{Bu}$. Main distances are shown in Å and relative free-energy to the resting state **2** (see Figure 3) is given in kcal mol⁻¹. For clarity, hydrogen atoms of ^tBu groups are omitted and carbon atoms of the oxidant are colored in light blue.



Scheme 4. Proposed heterolytic mechanism for the formation of the aldehyde product (dehydrogenation) pathway catalyzed by 1-^tBu. Relative Gibbs free-energies are given in parenthesis in kcal mol⁻¹.

for this process (25.7 kcal mol⁻¹) is lower than that for epoxidation (27.2 kcal mol⁻¹). The hydrogen transfer step is highly exergonic and irreversible (reverse barrier of 53.6 kcal mol⁻¹). Then, the proton transfer from the cationic allylic alcohol intermediate forms a water molecule and the aldehyde product and regenerates catalytic species 2, as sketched in Scheme 4. It should be pointed out that the oxygen atoms from the siloxy ligands act as basic sites in close proximity to the metal center and can assist the transfer of highly mobile H⁺.

Table 3 compares the overall free-energy barriers for dehydrogenation to aldehyde and epoxidation as a function of the bulkiness of catalyst substituents (1-^tBu, 1-ⁱPr, and 1-ⁿPr). Both reactions lower continuously their overall free-energy barriers as catalyst bulkiness is reduced, but dehydrogenation is less sensitive to steric effects than epoxidation with energy spans of 1.2 and 4.5 kcal mol⁻¹, respectively. These trends explain the inversion of selectivity observed experimentally in going from R=^tBu to ⁿPr (Figure 2), further validating our

Table 3. Comparison of the influence of steric effects on the overall free energy barriers for dehydrogenation and epoxidation of 3-methyl-2-buten-1-ol.^[a]

Entry	Cat. (1-R)	ΔG^{\ddagger} dehydrogenation	ΔG^{\ddagger} epoxidation ^[b]
1	1- ^t Bu	25.7	27.2
2	1- ⁱ Pr	25.5	24.3
3	1- ⁿ Pr	24.5	22.7

[a] Gibbs free-energy barriers are given in kcal mol⁻¹. [b] Barriers associated to the fastest O-transfer pathway for each catalyst.

mechanistic proposal. In fact, the computed difference between free-energy barriers of the two reactions are in qualitative (if not quantitative) agreement with the experimental product distribution. The lower dependence of the dehydrogenation barriers on the steric hindrance can be rationalized by comparing the structures of the different transition states (see Figure S6). The epoxidation reaction involves the approach of the bulkiest part of the substrate to the OO^tBu moiety and takes place through a spiro-like transition state where the substituents of the alkene point towards the R groups of the catalyst. On the other hand, the dehydrogenation proceeds through TS_{ald}, in which only the -CH₂OH group of the substrate becomes close to the oxidant occupying the space between two Si(^tBu) groups and leaving the bulkier -CH=CH(CH₃)₂ part far away from the sterically crowded region.

It is worth reminding here that such changes in selectivity were not observed when using H₂O₂ as an oxidizing agent, selectivity for epoxide remaining high.^[13] In the present case, the environment provided by the SiloxPOM (size of the R substituent) discriminates the selectivity of the reaction. This highlights the fact that the nature of the oxidant (ROOH, R=H vs ^tBu) has an effect on the free-energy barriers of the oxidation reactions but also, and mainly, on the shape of the reactive intermediate that forms and on its accessibility by the organic substrates depending on the surrounding environment, i.e., here, the degree of confinement. These important issues have also been addressed in the case of Ti-containing zeolites (microporous or mesoporous). Pore size and nature of the surface, particularly hydrophobicity and hydrophilicity, are known to be key factors that influence the activity in epoxidation of alkenes (small linear, cyclic, or large organic molecules of interest for production of fine chemicals) when using either aqueous H₂O₂ or bulky organic hydroperoxides as oxidants.^[5,36–39]

We note that the formation of the aldehyde 3-methyl-2-butenal is also observed in the absence of Ti, using the SiloxPOM complex (THA)₃[SbW₉O₃₃(^tBuSiOH)₃] (see above). This result suggests that the redox-active behavior of the tungstate framework facilitates a one-electron oxidation of the substrate. To evaluate the feasibility of such process, we computed the Proton Coupled Electron Transfer (PCET) from the allylic alcohol substrate to the POM framework resulting in a radical allyl alcohol intermediate and the reduced, protonated complex [HSb(W^VW^{VI})₈O₃₃(^tBuSiOH)₃]³⁻. The products of this initial PCET event lie at thermally accessible energy levels ($\Delta G^{\circ} = +20.8$ kcal mol⁻¹), suggesting that such process may take place at the experimental conditions as long as the associated free-energy barrier is affordable. However, we must note that evaluating the kinetics of PCET steps is still a great challenge for computational chemistry and far beyond the scope of this work. After this, the formation of the aldehyde could proceed downhill through a series of proton and electron transfer steps (see Scheme S3 for further details) that could involve the generation of radical species such as ^tBuO• or [HSb(W^VW^{VI})₈O₃₃(^tBuSiOH)₃]³⁻. In this regard, experiments to intercept any radical species that could support our preliminary calculations are currently under way in our groups. This one-electron

oxidation mechanism may occur simultaneously to the heterolytic one for the 1-^tBu catalyst while for Ti-silicate catalysts there is not a redox-active structure analogous to the tungstate framework.

Epoxidation of unfunctionalized olefins

Epoxidation of unfunctionalized olefins was also investigated. Noteworthy, we observed that the conversion was completely inhibited when using the more crowded catalyst 1-^tBu (Table 4, entry 1). This correlates with the previous results on the oxidation of allylic alcohol with 1-^tBu for which neither an inner-sphere nor an outer-sphere were operative. Then, the results showed that the less bulky the substituent at the silicon atom, the more the conversion (Table 4, entries 2 and 3). This also correlates with the representations reported in Figure 1, which emphasize the impact of the steric surrounding on the reactant accessibility to the active confined sites, and thus on the conversion rate. The high selectivity towards epoxide (cyclic, terminal, trans- and cis-alkenes) confirms that a concerted mechanism occurs, in which the electrophilic O-transfer proceeds through a heterolytic pathway.^[20,21] Accordingly, the calculated free-energy cost of the homolytic activation of an allylic C–H bond by the POM framework in cyclohexene (28.6 kcal mol⁻¹) is higher than in an allylic alcohol (20.8 kcal mol⁻¹; *vide supra*) that contains a heteroatom in the α position that enhances the delocalization of the radical.

Calculations also support the experimental results as reported in Table 4 (last column). When moving to smaller R groups (from entry 1 to entry 3) the computed overall free-energy barrier for the O-transfer decreases accordingly. More, another consequence of the steric issues between the R substituents of the *tris*-grafted active species [SbW₉O₃₃(RSiO)₃Ti(η^2 -OO^tBu)]³⁻ and the incoming substrate is a higher conversion for a *cis* olefin rather than *trans* olefin: this is exemplified by the higher conversion obtained for the *cis*- β -methylstyrene compared to the *trans*- β -methylstyrene (entries 5 and 6 in Table 4). We can ascribe this trend to steric repulsions between one of the substituents of the alkene and the catalyst during substrate approach of the *trans*- β -methylstyrene, while for *cis*- β -methylstyrene both substituents can point towards the solvent during substrate approach, leading to a lower free-energy barrier.^[34]

Finally, a rather good activity was obtained for the epoxidation of linear terminal olefins (1-hexene, Table 4 entry 4), which are electron-deficient substrates and good models for propene.^[41] Also, in agreement with experimental trends, the free-energy barrier obtained for 1-hexene is higher than that for cyclohexene (Table 4, entry 4), which can be ascribed to the weaker nucleophilic character of the double bond ($E\pi_{C=C} = -9.31$ eV vs. -9.06 eV for 1-hexene and cyclohexene, respectively).

Conclusion

In the present work, we report on our studies on the oxidation of allyl alcohols and non-functionalized alkenes with *tert*-butyl hydroperoxide (TBHP), catalyzed by a family of titanium derivatives (THA)₃[(α -B-SbW₉O₃₃)(RSiO)₃Ti(OⁱPr)] (1-*R*). In comparison with our previous studies using H₂O₂, for which unproductive decomposition of the oxidant was observed, the use of TBHP enable to clearly demonstrate the effect of steric hindrance (*R* = ^tBu, ⁱPr, ⁿPr) on the efficiency and selectivity of the reaction.

In contact with TBHP we assume that an active titanium alkyl peroxide species forms, [(α -B-SbW₉O₃₃)(RSiO)₃Ti(η^2 -OO^tBu)]³⁻, similarly to the [Ti]-(η^2 -OOH) reported previously. Compared to H₂O₂, TBHP oxidant is less active towards epoxidation due to the steric repulsive interactions of bulky ^tBu group of the peroxide with the catalyst 1-*R*. A direct consequence when dealing with allylic alcohols as substrates is that the *outer-sphere* mechanism becomes competitive with the *inner-sphere* one [coordination of the allylic alcohol to the Ti center], causing a mechanistic shift as the bulkiness of catalyst substituents is reduced (Figure 6). This is nicely manifested in the selectivity for the epoxidation of geraniol by less bulky 1-ⁿPr catalyst, where a preference for oxidizing the non-functionalized double bond through the *outer-sphere* mechanism results in the larger formation of the 6,7-epoxy geraniol. In general, our calculations demonstrate that *outer-sphere* mechanism has a lower free-energy barrier in the case of the less bulky 1-ⁿPr catalyst.

For the first time, atomistic simulations have analyzed in the detail the side reaction yielding the aldehyde providing an explanation for the observed selectivity change as a function of catalyst bulkiness. The novel, proposed mechanism involves the *outer-sphere* heterolytic hydrogen transfer from the allylic

Table 4. Epoxidation of alkenes with TBHP, catalyzed by (THA)₃[SbW₉O₃₃(RSiO)₃Ti(OⁱPr)], R = ^tBu: 1-^tBu, R = ⁱPr: 1-ⁱPr, R = ⁿPr: 1-ⁿPr.^[a]

Entry	Cat.	Alkene	Conv ^[b] [%]	Epox [%]	Sel [%]	ΔG^\ddagger ^[d]
1	1- ^t Bu	cyclohexene	< 5	<i>n.a.</i> ^[c]		25.9
2	1- ⁱ Pr	cyclohexene	70	69.3	99	23.1
3	1- ⁿ Pr	cyclohexene	97	96.4	> 99	21.9
4	1- ⁿ Pr	1-hexene	46.5	46.2	> 99	23.5
5	1- ⁿ Pr	<i>trans</i> - β -methylstyrene	37.7	37.4	> 99	
6	1- ⁿ Pr	<i>cis</i> - β -methylstyrene	78.9	78.8	> 99	

[a] All reactions were carried out in acetonitrile at 65 °C with [catalyst] = 2.6 mM, [olefin]₀ = [TBHP]₀ = 0.26 M. [b] Conversion based on NMR analysis after 22 h of reaction. [c] The conversion is too low to ascertain the selectivity in epoxide. [d] Gibbs free-energy barrier for the O-transfer step in kcal mol⁻¹.

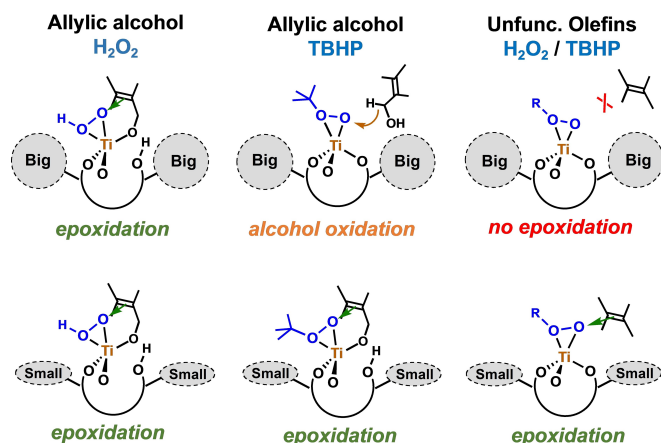


Figure 6. Influence of the size of the *R* substituents on the reaction pathway and product selectivity in the H_2O_2 or TBHP-based epoxidation of allylic alcohols and unfunctionalized alkenes, catalyzed by 1-*R*.

alcohol to the electrophilic α -oxygen of the peroxide, followed by proton transfer from the cationic allylic alcohol intermediate to yield the aldehyde product. The oxidation to aldehydes is less sensitive to the steric hindrance than epoxide reaction, therefore reducing the bulkiness of catalysts substituents ($R = \text{t-Bu}$, t-Pr , and n-Pr) lowers in larger extent the free-energy barrier of the epoxidation reaction increasing its activity and selectivity. Calculations also showed that the POM framework can promote the oxidative dehydrogenation of allylic alcohols to aldehydes acting as electron and proton acceptor, while TBHP acts as terminal oxidant. The novel, proposed mechanism proceeds through a sequence of one-electron oxidations via Proton Coupled Electron Transfer (PCET) events. Finally, catalyst design using TBHP oxidant demonstrates that reducing the bulkiness of the substituents in the silanol functions of the catalyst allows epoxidizing unfunctionalized alkenes. Structure-activity relationships can be built with the size of the substituents in the catalyst and the HOMO energies of the double bond for terminal alkenes.

Overall, these results show how activity and selectivity are intimately linked to the chemical surrounding, nature of reaction intermediates and pathways, and to the shape of the substrates. We have shown how Ti-SiloxPOM with tailored steric properties can become an interesting object to discriminate between different reaction paths by means of a confinement effect. A control of its properties could also allow to manage the regio- and stereochemistry of oxidation reactions.

Experimental Section

Computational details

DFT calculations were performed using the Gaussian16 rev. A03 software^[42] at $\omega\text{B97X-D}$ level of theory,^[43] which includes dispersion corrections to better account the non-covalent interactions involving the bulky t-Bu substituent of TBHP. The LANL2DZ basis set and associated pseudopotentials^[44] were used to describe W and Ti

centers whereas the remaining atoms were described by the all-electron 6-31G(d,p) basis set.^[45–47] Solvent effects of acetonitrile were included in geometry optimizations and energy calculations using the IEF-PCM implicit solvation model^[48] as implemented in Gaussian16. All minima were characterized by the lack of imaginary frequencies whereas only one imaginary frequency was identified for transition-state structures, which is associated to the normal mode of vibration connecting reactants and products. A data set collection of the optimized structures for the most representative species is available in the ioChem-BD repository and can be accessed via DOI: 10.19061/iochem-bd-2-47.^[49]

Materials and methods

The lacunary polyoxotungstate $\text{Na}_9[\alpha\text{-B-SbW}_9\text{O}_{33}]$, its silanol derivatives $(n\text{-Hex}_4\text{N})_3[(\alpha\text{-B-SbW}_9\text{O}_{33})(\text{RSiOH})_3]$ ($R = \text{t-Bu}$, t-Pr , n-Pr) and the titanium complexes $(n\text{-Hex}_4\text{N})_3[(\alpha\text{-B-SbW}_9\text{O}_{33})(\text{t-BuSiO})_3\text{Ti}(\text{O}^i\text{Pr})]$ (1- t-Bu), $(n\text{-Hex}_4\text{N})_3[(\alpha\text{-B-SbW}_9\text{O}_{33})(\text{t-PrSiO})_3\text{Ti}(\text{O}^i\text{Pr})]$ (1- t-Pr), $(n\text{-Hex}_4\text{N})_3[(\alpha\text{-B-SbW}_9\text{O}_{33})(\text{n-PrSiO})_3\text{Ti}(\text{O}^i\text{Pr})]$ (1- n-Pr), were prepared as reported in the literature.^[13] All manipulations were conducted under an inert atmosphere using standard Schlenk techniques and a Glovebox with purification system. *tert*-Butyl hydroperoxide (TBHP, 5.5 M in decane), was purchased from Aldrich and used as received. ^1H NMR spectra were obtained at room temperature in 5 mm o.d. tubes on a Bruker Avancell 300 spectrometer equipped with a QNP probehead or on a Bruker Avancell 600 spectrometer equipped with a BBFO probehead. For ^1H , chemical shifts are referenced with respect to tetramethylsilane by using the solvent signals as secondary standard. Elemental analyses were performed by the « Service de microanalyses » from the ICSN-CNRS, Gif-sur-Yvette, France.

Catalytic olefin epoxidation. In a screw capped Schlenk (equipped with a rotaflo type valve) were introduced under argon the catalyst (2.6 mM), dry acetonitrile, olefin (0.26 M) and *t*-butyl hydroperoxide (0.26 M). The mixture was stirred while heating at the desired temperature (343 K) for 22 h. Dilution by diethyl ether gave a turbid suspension from which the solid may be taken off (by filtration or centrifugation). Conversions were assigned by NMR analysis.

Monitoring by NMR: A screw capped 5 mm o.d. NMR tube under argon was charged with complex 1- n-Pr (4.9 mg, 1.31 μmol) and dry acetonitrile- d_3 (0.5 mL), alkene (130 μmol) and TBHP (5.5 M in decane, 23.5 μL , 130 μmol) were successively added to the mixture. Each step was monitored at 300 K by ^1H on a Bruker Avancell 600 spectrometer equipped with a BBFO probehead. The acquiring parameters (relaxation delays) have been optimized to ensure an accurate integration measurement.

Acknowledgements

T.Z. and G.G. acknowledge the Sorbonne University CSC program for a Ph.D. grant and the CNRS for generous support. J. J. C. and J.-M. P. thank the Spanish Ministry of Science (PGC2018-100780-B-I00 and CTQ2017-87269-P projects) for generous support.

Conflict of Interest

The authors declare no conflict of interest.

Keywords: titanium · oxidation · alkene · mechanistic study · DFT · polyoxotungstates

- [1] T. Katsuki, K. B. Sharpless, *J. Am. Chem. Soc.* **1980**, *102*, 5974–5976.
- [2] D. J. Berrisford, C. Bolm, K. B. Sharpless, *Angew. Chem. Int. Ed.* **1995**, *34*, 1059–1070; *Angew. Chem.* **1995**, *107*, 1159–1171.
- [3] G. Perego, G. Bellussi, C. Corno, M. Taramasso, F. Buonomo, A. Esposito, in *Studies in Surface Science and Catalysis*, **1986**, pp. 129–36.
- [4] I. W. C. E. Arends, R. A. Sheldon, M. Wallau, U. Schuchardt, *Angew. Chem. Int. Ed. Engl.* **1997**, *36*, 1144–1163.
- [5] O. A. Kholdeeva, *Catal. Sci. Technol.* **2014**, *4*, 1869–1889.
- [6] *Catalytic Oxidations with Hydrogen Peroxide as Oxidant*, (Ed.: G. Strukul), Kluwer Academic Publishers, Netherlands, **1992**.
- [7] M. G. Clerici, P. Ingallina, *J. Catal.* **1993**, *140*, 71–83.
- [8] T. Tatsumi, in *Modern Heterogeneous Oxidation Catalysis: Design, Reactions and Characterization*, Mizuno N., **2009**, pp. 125–155.
- [9] M. G. Clerici, M. E. Domine, in *Liquid Phase Oxidation via Heterogeneous Catalysis: Organic Synthesis and Industrial Applications*, John Wiley & Sons, Inc, **2013**, p. 21.
- [10] M. G. Clerici, *Kinet. Catal.* **2015**, *56*, 450–455.
- [11] C. P. Gordon, H. Engler, A. S. Tragl, M. Plodinec, T. Lunkenbein, A. Berkessel, J. H. Teles, A.-N. Parvulescu, C. Copéret, *Nature* **2020**, *586*, 708–713.
- [12] T. Zhang, L. Mazaud, L.-M. Chamoreau, C. Paris, A. Proust, G. Guillemot, *ACS Catal.* **2018**, *8*, 2330–2342.
- [13] A. Solé-Daura, T. Zhang, H. Fouilloux, C. Robert, C. M. Thomas, L.-M. Chamoreau, J. J. Carbó, A. Proust, G. Guillemot, J. M. Poblet, *ACS Catal.* **2020**, *10*, 4737–4750.
- [14] G. Guillemot, E. Matricardi, L.-M. Chamoreau, R. Thouvenot, A. Proust, *ACS Catal.* **2015**, *5*, 7415–7423.
- [15] T. Zhang, A. Solé-Daura, S. Hostachy, S. Blanchard, C. Paris, Y. Li, J. J. Carbó, J. M. Poblet, A. Proust, G. Guillemot, *J. Am. Chem. Soc.* **2018**, *140*, 14903–14914.
- [16] C. W. Yoon, K. F. Hirsekorn, M. L. Neidig, X. Yang, T. D. Tilley, *ACS Catal.* **2011**, *1*, 1665–1678.
- [17] H. C. L. Abbenhuis, *Chem. Eur. J.* **2000**, *6*, 25–32.
- [18] L. Zhang, H. C. L. Abbenhuis, G. Gerritsen, N. N. Bhriani, P. C. M. M. Magusin, B. Mezari, W. Han, R. A. van Santen, Q. Yang, C. Li, *Chem. Eur. J.* **2007**, *13*, 1210–1221.
- [19] C. Copéret, A. Comas-Vives, M. P. Conley, D. P. Estes, A. Fedorov, V. Mougel, H. Nagae, F. Núñez-Zarur, P. A. Zhizhko, *Chem. Rev.* **2016**, *116*, 323–421.
- [20] N. S. Antonova, J. J. Carbó, U. Kortz, O. A. Kholdeeva, J. M. Poblet, *J. Am. Chem. Soc.* **2010**, *132*, 7488–7497.
- [21] S. E. Jacobson, D. A. Muccigrosso, F. Mares, *J. Org. Chem.* **1979**, *44*, 921–924.
- [22] C. Aubry, G. Chottard, N. Platzer, J. M. Bregeault, R. Thouvenot, F. Chauveau, C. Huet, H. Ledon, *Inorg. Chem.* **1991**, *30*, 4409–4415.
- [23] H. Mimoun, *Angew. Chem. Int. Ed.* **1982**, *21*, 734–750; *Angew. Chem.* **1982**, *94*, 750–766.
- [24] C. Venturello, R. D'Aloisio, J. C. J. Bart, M. Ricci, *J. Mol. Catal.* **1985**, *32*, 107–110.
- [25] J.-M. Brégeault, M. Vennat, S. Laurent, J.-Y. Piquemal, Y. Mahha, E. Briot, P. C. Bakala, A. Atlamsani, R. Thouvenot, *J. Mol. Catal. A* **2006**, *250*, 177–189.
- [26] D. V. Deubel, G. Frenking, P. Gisdakis, W. A. Herrmann, N. Rösch, J. Sundermeyer, *Acc. Chem. Res.* **2004**, *37*, 645–652.
- [27] K. Kamata, M. Kotani, K. Yamaguchi, S. Hikichi, N. Mizuno, *Chem. - Eur. J.* **2007**, *13*, 639–648.
- [28] N. V. Maksimchuk, I. D. Ivanchikova, G. M. Maksimov, I. V. Eltsov, V. Yu. Evtushok, O. A. Kholdeeva, D. Lebbie, R. J. Errington, A. Solé-Daura, J. M. Poblet, J. J. Carbó, *ACS Catal.* **2019**, *9*, 6262–6275.
- [29] N. V. Maksimchuk, G. M. Maksimov, V. Yu. Evtushok, I. D. Ivanchikova, Y. A. Chesalov, R. I. Maksimovskaya, O. A. Kholdeeva, A. Solé-Daura, J. M. Poblet, J. J. Carbó, *ACS Catal.* **2018**, *8*, 9722–9737.
- [30] I. Y. Skobelev, V. Yu. Evtushok, O. A. Kholdeeva, N. V. Maksimchuk, R. I. Maksimovskaya, J. M. Ricart, J. M. Poblet, J. J. Carbó, *ACS Catal.* **2017**, *7*, 8514–8523.
- [31] P. Jiménez-Lozano, I. Y. Skobelev, O. A. Kholdeeva, J. M. Poblet, J. J. Carbó, *Inorg. Chem.* **2016**, *55*, 6080–6084.
- [32] I. Y. Skobelev, O. V. Zalomaeva, O. A. Kholdeeva, J. M. Poblet, J. J. Carbó, *Chem. - Eur. J.* **2015**, *21*, 14496–14506.
- [33] P. Jiménez-Lozano, I. D. Ivanchikova, O. A. Kholdeeva, J. M. Poblet, J. J. Carbó, *Chem. Commun.* **2012**, *48*, 9266–9268.
- [34] B. G. Donoeva, T. A. Trubitsina, N. S. Antonova, J. J. Carbó, J. M. Poblet, G. Al-Kadamany, U. Kortz, O. A. Kholdeeva, *Eur. J. Inorg. Chem.* **2010**, *2010*, 5312–5317.
- [35] F. Maspero, U. Romano, *J. Catal.* **1994**, *146*, 476–482.
- [36] T. Blasco, A. Corma, M. T. Navarro, J. P. Pariente, *J. Catal.* **1995**, *156*, 65–74.
- [37] A. Corma, P. Esteve, A. Martínez, *J. Catal.* **1996**, *161*, 11–19.
- [38] D. T. Bregante, D. W. Flaherty, *ACS Catal.* **2019**, *9*, 10951–10962.
- [39] D. T. Bregante, J. Z. Tan, R. L. Schultz, E. Z. Ayla, D. S. Potts, C. Torres, D. W. Flaherty, *ACS Catal.* **2020**, *10*, 10169–10184.
- [40] F. Di Furia, G. Modena, *Pure Appl. Chem.* **1982**, *54*, 1853–1866.
- [41] M. G. Clerici, G. Bellussi, U. Romano, *J. Catal.* **1991**, *129*, 159–167.
- [42] M. J. Frisch, G. W. Trucks, H. B. Schlegel, G. E. Scuseria, M. A. Robb, J. R. Cheeseman, G. Scalmani, V. Barone, G. A. Petersson, H. Nakatsuji, X. Li, M. Caricato, A. V. Marenich, J. Bloino, B. G. Janesko, R. Gomperts, B. Mennucci, H. P. Hratchian, J. V. Ortiz, A. F. Izmaylov, J. L. Sonnenberg, Williams, F. Ding, F. Lipparini, F. Egidi, J. Goings, B. Peng, A. Petrone, T. Henderson, D. Ranasinghe, V. G. Zakrzewski, J. Gao, N. Rega, G. Zheng, W. Liang, M. Hada, M. Ehara, K. Toyota, R. Fukuda, J. Hasegawa, M. Ishida, T. Nakajima, Y. Honda, O. Kitao, H. Nakai, T. Vreven, K. Throssell, J. A. Montgomery Jr., J. E. Peralta, F. Ogliaro, M. J. Bearpark, J. J. Heyd, E. N. Brothers, K. N. Kudin, V. N. Staroverov, T. A. Keith, R. Kobayashi, J. Normand, K. Raghavachari, A. P. Rendell, J. C. Burant, S. S. Iyengar, J. Tomasi, M. Cossi, J. M. Millam, M. Klene, C. Adamo, R. Cammi, J. W. Ochterski, R. L. Martin, K. Morokuma, O. Farkas, J. B. Foresman, D. J. Fox, *Gaussian 16 Rev. A.03*, Wallingford, CT, **2016**.
- [43] J.-D. Chai, M. Head-Gordon, *Phys. Chem. Chem. Phys.* **2008**, *10*, 6615–6620.
- [44] P. J. Hay, W. R. Wadt, *J. Chem. Phys.* **1985**, *82*, 270–283.
- [45] M. M. Francl, W. J. Pietro, W. J. Hehre, J. S. Binkley, M. S. Gordon, D. J. DeFrees, J. A. Pople, *J. Chem. Phys.* **1982**, *77*, 3654–3665.
- [46] P. C. Hariharan, J. A. Pople, *Theor. Chim. Acta* **1973**, *28*, 213–222.
- [47] W. J. Hehre, R. Ditchfield, J. A. Pople, *J. Chem. Phys.* **1972**, *56*, 2257–2261.
- [48] E. Cancès, B. Mennucci, J. Tomasi, *J. Chem. Phys.* **1997**, *107*, 3032–3041.
- [49] M. Álvarez-Moreno, C. de Graaf, N. López, F. Maseras, J. M. Poblet, C. Bo, *J. Chem. Inf. Model.* **2015**, *55*, 95–103.

Manuscript received: November 1, 2020
Revised manuscript received: November 27, 2020
Accepted manuscript online: December 9, 2020
Version of record online: January 22, 2021